Light & Engineering
Vol. 28, No. 5, pp. 9–24, 2020

https://doi.org/10.33383/2020-018
Svetotekhnika #4 pp.64–76

BRIGHTNESS IN THE PHOTOPIC RANGE: PSYCHOPHYSICAL MODELLING WITH BLUE-SENSITIVE RETINAL SIGNALS

Peter Bodrogi, Xue Guo, and Tran Quoc Khanh

Laboratory of Lighting Technology, Technische Universität Darmstadt, Darmstadt, Germany
Email: bodrogi@lichttechnik.tu-darmstadt.de

ABSTRACT

The brightness perception of a large (41°) uniform visual field was investigated in a visual psychophysical experiment. Subjects assessed the brightness of 20 light source spectra of different chromaticities at two luminance levels, L_v=267.6 cd/m^2 and L_v=24.8 cd/m^2. The resulting mean subjective brightness scale values were modelled by a combination of the signals of retinal mechanisms: *S*-cones, rods, intrinsically photosensitive retinal ganglion cells (*ipRGCs*) and the difference of the *L*-cone signal and the *M*-cone signal. A new quantity, "relative spectral blue content", was also considered for modelling. This quantity was defined as "the spectral radiance of the light stimulus integrated with the range (380–520) nm, relative to luminance". The "relative spectral blue content" model could describe the subjective brightness perception of the observers with reasonable accuracy.

Keywords: subjective brightness, brightness perception, photopic brightness model, retinal mechanisms, spectral blue content

1. INTRODUCTION

1.1. Brightness: Definition and Relevance

Brightness (that is, the subjective brightness impression of a visual stimulus as perceived by human observers) is defined in the International Lighting Vocabulary of the International Commission on Illumination, CIE ILV) as an "attribute of a visual perception according to which an area appears to emit or reflect more or less light" [1]. Although brightness has "at least three aspects" [2], the present article deals only with the so-called "spatial brightness" aspect, the perception of "the overall amount of light reaching the observer's eyes" [2]. The concept of "spatial brightness" is important in many areas of lighting engineering, including the design of a lit interior space, in which brightness should be generally high enough in order "to make seeing easy" [3], that is, for good visual performance. The spatial brightness distributions of interior lighting should be well-balanced for good visual comfort and good (three-dimensional) space perception or perceived spaciousness [3, 4]. With exterior lighting, increasing the perceived spatial brightness of a scene increases the impression of safety [6], which is important for pedestriansy. The concept of spatial brightness refers to the brightness of spatially extended scenes, rather than small light sources or small individual objects [5, 7].

1.2. The Difference Between Brightness and Luminance

In 1933, L.A. Jones was appointed the Chairman of the Optical Society of America Committee on Colourimetry (1922) and asked to update recent work progress. Subsequently, a preliminary report was published, in which the term luminance was introduced [8]. Afterwards, Jones wrote [9] that the Committee recommended that the word 'luminosity' be substituted for 'visibility'. The Committee also decided to reserve the term 'brightness' as the name for the sensory attribute correlated with the photometric quantity to which the term 'luminance' was assigned. Later it was stated that "photometry was based on an incomplete description of the human visual system's capabilities" [10], because the $V(\lambda)$ function (the basis of photometry) and its derived quantities (luminance, illuminance, etc.) represent the linear combination of only the long- (*L*-) and medium- (*M*-) wavelength sensitive retinal cone photoreceptors and do not include the important signals of the short-wavelength sensitive (*S*-) cones, rod photoreceptors, and intrinsically photosensitive retinal ganglion cells (*ipRGCs*).

The latter (so-called "shorter-wavelength sensitive") photoreceptor signals contribute (depending on the luminance level) to the brightness perception [11–17] together with the signals of the two chromatic (opponent) channels, $(L–M)$ and $(L+M\text{-}S)$ [13]. A saturated colour stimulus looks brighter than its de-saturated counterpart of the same luminance (this is the "brightness-luminance discrepancy" or Helmholtz-Kohlrausch effect) [18, 19]. Thus, the impression of brightness cannot be described by the quantity "luminance" alone. In the above description, the term "signal" is understood mathematically in the sense of weighting the relative spectral power distribution of the light source with the spectral sensitivity of a photoreceptor and integrating in the visible wavelength range.

1.3. Brightness Models

Here, selected brightness models from the literature are summarized and compared with the models used in the present article. Brightness models usually combine the values of the abovementioned retinal signals, including the two opponent channels ($(L–M)$ and $(L+M\text{-}S)$), or their approximations based on the *XYZ* tristimulus values of standard CIE colourimetry. Brightness models also contain an approximation of the $(L+M)$ signal (most often photopic luminance, L_v is used), a representation of the rod signal (most often scotopic luminance is used), and the *ipRGC* signal (the signal of the intrinsically photosensitive retinal ganglion cells) in order to derive a numeric predictor quantity for human brightness impression. In some models, this predictor quantity is only intended to forecast the rank order of the visual stimuli according to their brightness perception, without representing a numeric correlate of the absolute magnitude of perceived brightness. These are the so-called equivalent luminance (or L_{eq}) models. Eq. 1 shows an example of a brightness model according to Fotios and Levermore [20]:

$$L_{eq} = L_v \cdot (S/V)^{0.24}, \tag{1}$$

where the *S*-signal is computed by the Smith and Pokorny cone sensitivity data [21] and the quantity *V* (so-called *V*-signal) is obtained by weighting the relative spectral power distribution of the light source with the $V(\lambda)$ function and integrating in the visible wavelength range.

Another example of a brightness model is "equivalent luminance L_{eq} according to Ware and Cowan" (also called WCCF equation) [22]. This model is based on standard CIE colourimetry and shown below

$$L_{eq} = (B/L) \cdot L_v, \tag{2}$$

where the symbol (B/L) represents the so-called "brightness-luminance ratio" to be computed from the CIE *x*, *y* chromaticity coordinates of the stimulus by

$$lg(B/L) = 0.256 - 0.184 \cdot y - 2.527 \cdot x \cdot y + \\ +4.656 \cdot x^3 \cdot y + 4.657 \cdot x \cdot y^4. \tag{3}$$

Rea et al. (2011) model [15] works with the weighted sum of two signals: the *V*-signal and the *S*-signal. In Fotios and Levermore (1998) model [13], "perceived brightness is considered to be a sum of the total activity in three channels": $(L+M)$ (represented by $V(\lambda)$) and the above-mentioned two opponent channels. The Guth model [23] is based on the concept of vector luminance that equals the square root of three squared components, *A* (achromatic component), *T* (first chromatic component) and *D* (second chromatic component). Yaguchi and Ikeda (1983) used a modification of the Guth model to account for the spectral additivity failure that they measured in their visual brightness matching experiments [24]. Kokoschka-Bodmann model [25, 26] computes the value of equivalent luminance for brightness from the 10° tristimulus values (X_{10}, Y_{10}, Z_{10}) and scotopic luminance (L').

In the Yamakawa et al. model [47], obtained as a result of a subjective brightness magnitude estimation experiment, is shown below:

$$R = 0.00484 \cdot G^{1.1} + 2.31 \cdot E^{0.48}, \tag{4}$$

Table 1. Overview of Brightness Models Given in the Literature and Proposed in this Article

The authors of the models	Model type	Signals or quantities
Fotios and Levermore [20] (1)	Equivalent luminance	S, V, L_v
Ware and Cowan (*WCCF*) [22] (2, 3)	Equivalent luminance	x, y, L_v
Rea et al. [15]	Weighted sum of signals	S, V
Fotios and Levermore [13]	Weighted sum of channels	$L+M, L–M, L+M-S$
Guth [23]	Weighted sum of channels	A, T, D
Yaguchi and Ikeda [24]	Weighted sum of channels	A, T, D (modified)
Kokoschka-Bodmann[25, 26]	Equivalent luminance	X_{10}, Y_{10}, Z_{10}, L' (rods)
Besenecker and Bullough's "B_2"[14]	Weighted sum of signals	*S, V, ipRGC*
Yamakawa et al. [47] (4)	Weighted sum of channels	*E*, *ipRGC*
Present article, Eq. (13)	Relative spectral blue content	L_v, $\Phi_{rel,\ blue}$

where the *ipRGC* signal (this was called melanopsin signal on the retina, denoted by *G*) was combined with retinal illuminance (denoted by *E*) to predict the perceived brightness (denoted by *R*) of metameric white stimuli (at the fixed chromaticity of x=0.328 and y=0.367) with different amounts of the ipRGC signal and at different luminance levels (between 22 cd/m^2 and 112 cd/m^2).

Besenecker and Bullough's (2016) so-called "B_2 brightness model" [14] contains the weighted sum of three signals, the *V*-signal, the *S*-signal and the *ipRGC* signal, reflecting the fact that "short-wavelength (<500 nm) output of light sources enhances spatial brightness perception in the low-to-moderate photopic range". Inspired by this idea, in the present article the so-called relative spectral blue content will be considered as a new modelling quantity, and its definition is shown below:

$$\Phi_{rel,blue} = [267.6 / L_v] \cdot \int_{380}^{520} L_e(\lambda) d\lambda, \qquad (5)$$

where $\Phi_{rel,\ blue}$ is relative spectral blue content. It is defined as the spectral radiance $Le(\lambda)$ of the stimulus integrated between 380 nm and 520 nm, relative to its luminance L_v. This definition uses 267.6 cd/m^2 for re-scaling because this was one of the two luminance levels in the experimental method of the present article.

As mentioned above, the quantity of $\Phi_{rel,\ blue}$ is similar to Besenecker and Bullough's [14] concept of short-wavelength (<500 nm) output, but we use 520 nm as the upper limit in (5) in order to overlap slightly more with rod photoreceptor spectral sensitivity (to be able to better account for possible rod contribution). Table 1 shows a classification of the abovementioned brightness models according to the type of brightness model.

1.4. Objectives of the Present Article

In the present article, a visual brightness experiment will be described. The experiment was conducted at two fixed luminance levels (L_v=267.6 cd/m^2 and 24.8 cd/m^2) with 20 different chromaticities (different photoreceptor signal contents) of the visual stimulus at each level. The result will be modelled:

1. With a combination of the abovementioned signals of the retinal mechanisms;
2. With *relative spectral blue content* (5), as a proxy of the signals of the three shorter-wavelength sensitive mechanisms, *S*-cones, *ipRGCs,* and rods.

The research questions of the present article are:

1. Are the contributions of three shorter-wavelength mechanisms (*S*-cones, *ipRGCs* and, rods) to evoke human brightness perception distinguishable from each other (and from the relative spectral blue content) based on the results of the visual brightness experiment?
2. Is there significant rod contribution to perceived brightness at the two luminance levels of the experiment (L_v=267.6 cd/m^2 and 24.8 cd/m^2)?
3. Does the opponent signal (*L–M*) have an effect (the difference of the *L*-cone signal and the *M*-cone signal)?
4. Can we use the quantity of "relative spectral blue content*"* (5) to model the perceived brightness in a new, practicable model?

We will use a combination of the photoreceptor signals and relative spectral blue content for modelling brightness, i.e. to explain the subjective visual brightness scales (*VBS*) of the observers resulting from the experiment of the present article. These two hypotheses are formulated below:

$$VBS \sim lg\left(L_v\right)\cdot[A_S\left(S_{rel}\right)^{\gamma} + A_{ipRGC}\left(ipRGC_{rel}\right)^{\gamma} + \\ + A_R\left(R_{rel}\right)^{\gamma} + A_{L-M}\left(\left| L_{rel} - M_{rel}\right|\right)^{\gamma}], \quad (6)$$

$$VBS \sim lg\left(L_v\right)\cdot[(\Phi_{rel,blue})^{\gamma}]. \quad (7)$$

Eq. 6 represents signal combination formula, and eq. 7 is relative spectral blue content formula. Optimum model parameters (the signal weighting factors A_S, A_{ipRGC}, A_R, A_{L-M} and the exponent γ) will be calculated based on the mean brightness scales of the observers. The quantity $lg(L_v)$ is included to account for the effect of the changing overall luminance level of the visual stimulus. Here the "~" symbol means that the quantity on the left shall be explained by the quantity on the right. The quantity $|L_{rel}\text{-}M_{rel}|$ is a so-called opponent signal: the difference of the relative *L*-cone signal and the relative *M*-cone signal.

The so-called relative signal values L_{rel}, M_{rel}, S_{rel}, R_{rel} and $ipRGC_{rel}$ in (6) were computed as follows:

1. The spectral power distribution (SPD) of the stimulus was normalized so that its luminance equalled 267.6 cd/m²;

2. This normalized SPD was weighted by the relative spectral sensitivity of a certain retinal mechanism;

3. This weighted SPD was integrated in the wavelength range (380–780) nm.

This computation is shown below in (8) – (12):

$$L_{rel} = [267.6 / L_v] \cdot \int_{380}^{780} L_e(\lambda)L(\lambda)d\lambda, \quad (8)$$

$$M_{rel} = [267.6 / L_v] \cdot \int_{380}^{780} L_e(\lambda)M(\lambda)d\lambda, \quad (9)$$

$$S_{rel} = [267.6 / L_v] \cdot \int_{380}^{780} L_e(\lambda)S(\lambda)d\lambda, \quad (10)$$

$$R_{rel} = [267.6 / L_v] \cdot \int_{380}^{780} L_e(\lambda)V'(\lambda)d\lambda, \quad (11)$$

$$ipRGC_{rel} = [267.6 / L_v] \cdot \int_{380}^{780} L_e(\lambda)ipRGC(\lambda)d\lambda, \quad (12)$$

where the so-called "Stockman and Sharpe (2000) 2° fundamentals" [27, 28] were taken as the spectral sensitivities of the *L*-, *M*- and *S*-cones, $L(\lambda)$, $M(\lambda)$ and $S(\lambda)$. The spectral sensitivity of the intrinsically photosensitive retinal ganglion cells mechanism, $ipRGC(\lambda)$, was computed according to [29, 30], while the $V'(\lambda)$ function (the CIE scotopic spectral luminous efficiency function) was applied to represent the contribution of the rod photoreceptors to brightness perception.

Another purpose of the present article is to compare the optimum values of the exponent γ in (6) – (7) in case of the two luminance levels, 267.6 cd/m² and 24.8 cd/m², and to compare these optimum exponent values with the exponent value in Fotios and Levermore model (1) (γ =0.24). Another question is whether the two exponents at the two luminance levels of the present brightness experiment are significantly different. In summary, the objective of the present article is the modelling of the dataset of the new visual brightness experiment (see section 2) using hypothetical (6) and (7).

2. EXPERIMENTAL METHOD

The so-called brightness discrimination procedure [31] was used, during which the subjects were instructed to report which chamber of a two-chamber viewing booth appeared brighter, see Fig. 1. The subjects also had to tell how much brighter it was. To do this, they used the following ordinal scale: 0- almost equally bright, with almost no visible brightness difference; 1- somewhat brighter with a very small difference; 2- somewhat brighter; 3- explicitly brighter; and 4- explicitly brighter with a big difference. Then the subjects were instructed as follows: "if you say, for example, 'right 2', this means that the right chamber is somewhat brighter than the left chamber. If you say, 'left 4', this means that the left chamber is explicitly brighter than the right chamber and a big difference is visible." The investigator recorded every spoken answer immediately to a computer spreadsheet.

The subjects had a controlled sitting position in front of the viewing booth. This was checked by the experimenter. They had to sit in the middle so that the distance between the eyes and the viewing booth equalled 20 cm, and the distance between the eyes and the middle of the bottom of each chamber equalled 80 cm (see Fig. 1). The width of each chamber was 60 cm (corresponding to 41°), their height was 53 cm and their depth was 67 cm. The width of the separating wall between the two chambers equalled 6 cm (corresponding to 4°). The two light sources were positioned on the top of the viewing booth at a height of 72 cm above the top cov-

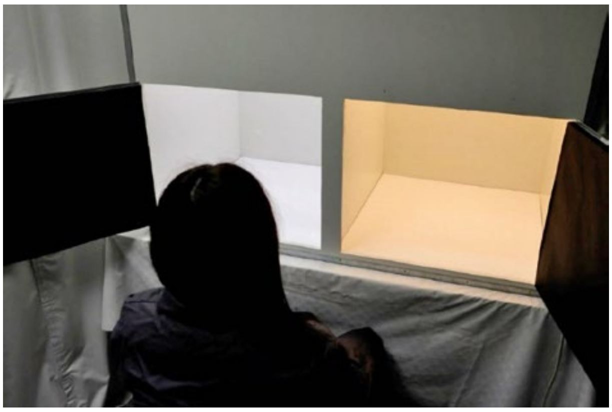

Fig. 1. The subject compared the brightness of the two chambers when the luminance of the two chambers was the same, i.e. at equi-luminance, either at 267.6 cd/m^2 or at 24.8 cd/m^2; here, the reference stimulus appears on the left ("2nd series")

ers of the two chambers. This provided ample space to mix the rays from the light sources for a uniform illumination at the bottom of the chambers. The uniformity was increased by two diffuser plates (one below the light sources and another one at the top covers of the chambers), so that the percentage of luminance differences on the bottom of the chambers was less than 3 %.

In the experiment, there was a reference stimulus: a phosphor-converted LED light source with a fixed relative spectral power distribution at 3991 K. This reference appeared either on the right (this is the definition of the "1st series") or on the left (this is the definition of the "2nd series") to counterbalance for possible "position bias" [31]. Each one of the two series was carried out twice at two separate occasions (called sessions): first with all stimuli at 267.6 cd/m^2 and second with all stimuli at 24.8 cd/m^2, so that there were four sessions in total. One observer carried out only one session on a given day, and one observer completed only one session (there were no repetitions). Subjects were always told whether the reference was on the left or on the right. They were also told that the reference would be the same during the whole session of comparisons with twenty test stimuli.

Before each session, a training phase was conducted in which each of the twenty test stimuli was shown in random order (10 s each) compared to the constant reference stimulus. The subjects did not have to answer in the training phase, they just had to consider a possible answer. During the training phase, in addition to the twenty test stimuli, two anchor stimuli were also shown in combination with the reference stimulus three times. One of the anchors was explicitly brighter (330 cd/m^2 and 33 cd/m^2 in case of the two luminance levels, respectively, with the relative spectrum No. 20 in Table 2) and the other one was explicitly darker (49 cd/m^2 and 5 cd/m^2, with the relative spectrum No. 6 in Table 2) than the reference stimulus (with a clearly visible brightness difference), and the subject was informed about this. The two anchors were shown first at the beginning, then after the 10th test stimulus, and finally at the end.

In the main part of each session, after 15 minutes of initial adaptation to the reference stimulus, the subject viewed the two chambers (reference and test) for 40 s. Then an automatic computer sound said: "please assess". Subsequently, the subject had to answer within 20 s. Before the next test stimulus appeared, the neutral white dark anchor stimulus was always displayed for 40 s, and the automatic sound informed the subject about this. During each 40 s interval, subjects were instructed to compare the brightness of the two stimuli as follows:

1. Consider the two bottoms only, and not the vertical walls;
2. Move your head slowly between the two chambers, looking at the two bottoms at least for 2 s each.

Stimuli with strong chromatic content (for example, the yellowish one in the right chamber in Fig. 1) evoked afterimages, but this effect was mitigated by the neutral white dark anchor stimulus displayed for 40 s between any subsequent test stimulus. The role of this recurrent dark anchor stimulus was not only to clear the afterimages, but also to restart the brightness discrimination procedure of the subject from the "explicitly darker" anchor.

Twenty test stimuli were always shown in random order to avoid the so-called "order effect" [31]. They were generated by an 11-channel LED light engine at two luminance levels: either at 267.6 (mean) ± 0.8 (STD) cd/m^2 or at 24.8 (mean) ± 0.07 (STD) cd/m^2. The 20 test stimuli had the same relative spectral power distributions at both luminance levels. This was ensured by an achromatically transmitting hole pattern positioned below the light engine. One of the test stimuli (No. 16 null condition stimulus) was optimized to have a similar relative $|L–M|$, S, rod and *ipRGC* signal values to the reference stimulus (see Table 2). Other test stimuli were designed (by optimizing the driving values of the 11 channels) to have different combinations of $|L–M|$,

Table 2. Signal Values of the 20 Test Stimulus and the Reference Stimulus

No.	L_v(cd/m^2)	$\lvert L_{rel}$-$M_{rel}\rvert$	L_{rel}	M_{rel}	S_{rel}	R_{rel}	$ipRGC_{rel}$	$\Phi_{rel,\ blue}$	Intent of optimization
1	268.2	0.001	0.386	0.387	0.024	0.345	0.211	0.188	rods high
2	267.4	0.168	0.453	0.285	0.015	0.155	0.080	0.058	$\lvert L–M\rvert$ high
3	268.3	0.108	0.431	0.322	0.034	0.269	0.171	0.158	rods high
4	267.7	0.088	0.440	0.352	0.331	0.525	0.586	0.740	rods and *ipRGC* high
5	268.1	0.083	0.431	0.348	0.436	0.327	0.426	0.703	*S* high
6	266.8	0.168	0.454	0.286	0.048	0.167	0.109	0.100	warm white
7	266.8	0.033	0.413	0.380	0.343	0.476	0.512	0.652	cool white
8	268.9	0.099	0.431	0.332	0.166	0.322	0.289	0.409	neutral white
9	268.4	0.101	0.433	0.332	0.144	0.292	0.268	0.307	balanced signals with higher *ipRGC*
10	268.0	0.167	0.452	0.285	0.018	0.157	0.083	0.062	$\lvert L–M\rvert$ high
11	266.7	0.037	0.415	0.377	0.380	0.477	0.530	0.793	cool white with higher local maxima
12	267.6	0.101	0.429	0.328	0.122	0.294	0.226	0.233	balanced signals with higher rods
13	267.1	0.042	0.426	0.384	0.831	0.538	0.767	1.164	very high *S*
14	268.0	0.095	0.427	0.332	0.150	0.274	0.223	0.238	balanced signals with higher *S*
15	267.4	0.097	0.430	0.333	0.134	0.293	0.253	0.274	neutral white
16	268.0	**0.101**	0.431	0.330	**0.131**	**0.281**	**0.237**	**0.250**	**null condition stimulus**
17	267.9	0.030	0.412	0.382	0.351	0.483	0.514	0.626	*ipRGC* high
18	267.1	0.168	0.455	0.287	0.051	0.206	0.143	0.142	warm white with higher local maxima
19	267.3	0.159	0.459	0.300	0.327	0.300	0.338	0.414	balanced signals with higher *S*
20	266.8	0.069	0.422	0.352	0.194	0.362	0.338	0.381	cool white
Ref.	270.3	**0.100**	0.431	0.331	**0.133**	**0.282**	**0.239**	**0.252**	neutral white (no optimization)

Note to Table 2: test stimulus No. 16 is the null condition stimulus. The reference light source was a phosphor-converted LED light source with a fixed relative spectral power distribution, see Fig. 2.

S, rod and *ipRGC* signal values, while maintaining the luminance level constant. Fig. 2 shows the relative spectral power distributions of the stimuli. Table 2 shows their L_{rel}, M_{rel}, S_{rel}, $|L_{\mathrm{rel}}$-$M_{\mathrm{rel}}|$, S_{rel}, R_{rel} (rod) and *ipRGC* signal values computed according to (8) – (12) and the optimization intent as a comment. Their relative spectral blue content value (5) is also shown in Table 2.

As for the reproducibility of the LED light engine's twenty SPDs, the change of luminance within the 40 days' experimental period was less than 1 %. The change of luminance of the reference light source was less than 1.5 %. The change of the L_{rel}, M_{rel}, R_{rel} (rod) and $ipRGC_{rel}$ signals was less than 1.5 % (for both the test stimuli and the reference). The change of the S_{rel} signal was less than 2.3 % (for both the test stimuli and the reference).

There were 25 participants in the 1st series (aged between 21 and 47 years, mean: 26.9; 10 Chinese, 1 Taiwanese, 9 Europeans, 2 Vietnamese, and 3 from the Middle East) and 21 participants in the 2nd series (aged between 21 and 47 years, mean: 27.4; 10 Chinese, 1 Taiwanese, 7 Europeans, 1 Vietnamese, and 2 from the Middle East), partially overlapping between the 1st and the 2nd series. All subjects had normal colour vision tested by the *Standard Pseudoisochromatic Plates for Acquired Colour Vision Defects*, Part II [32] and the *Desaturated Panel d-15* [33].

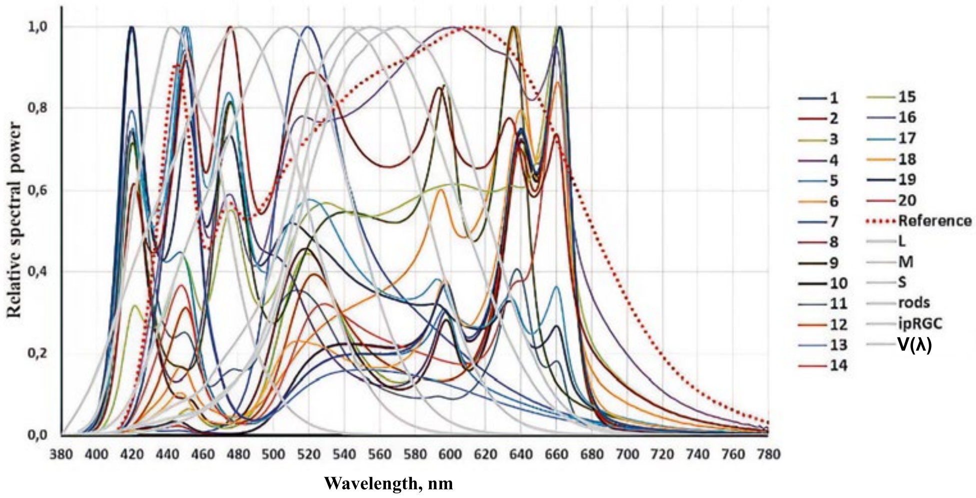

Fig. 2. Relative spectral power distributions of the 20 test stimuli, the reference stimulus, and relative spectral sensitivities of the *L, M, S,* rod, *ipRGC* mechanisms

3. RESULTS, MODELLING, AND DISCUSSION

In each session, the ordinal scale rating of every observer (i.e. an integer number between 0 and 4) was recorded for every one of the 20 test stimuli. If the reference was found to be darker (brighter) than the test stimulus, then the rating of that test stimulus was assigned a positive (negative) sign. Table 3 contains the average values and the average absolute deviation values (a measure of scatter among the observers) for the brightness ratings of all observers. The 20 test stimuli (see Table 2 and Fig. 2) are re-sorted in Table 3 according to their relative blue spectral content ($\Phi_{rel,\ blue}$) in descending order.

As can be seen from the last row of Table 3, the average value of the average absolute deviation value for all participating observers of all test stimuli equals to 1 rating unit in each series (1 and 2) and each luminance level (267.6 cd/m^2 and 24.8 cd/m^2). This (i.e. 1 rating unit of evaluation) is a characteristic value for the inter-observer variability of the result. Fig. 3 shows the average brightness scale values of Table 3.

As can be seen from Fig. 3, the average brightness ratings of all observers participating in each series show a downward trend with a decrease in the relative spectral content of blue. The test stimulus No. 13 with the highest relative spectral blue content value, $\Phi_{rel,\ blue}$ = 1.164, was the brightest. Overall, the last five test stimuli in Table 3 (No. 3, 18, 6, 10, and 2), having the lowest relative spectral blue content ($\Phi_{rel,\ blue}$ < 0.16), were the darkest. Spearman's correlation coefficient between the average brightness difference rating values of the two luminance levels equalled 0.944 for the first series and 0.916 for the second series. Both correlation coefficient values were significant (*T*-test, p<0.0001). This means that the two luminance levels exhibit similar brightness rating tendencies across all 20 test stimuli. The correlation between the brightness ratings of the two series was also high: Spearman's correlation coefficient equalled 0.911 (at 267.6 cd/m^2) and 0.838 (at 24.8 cd/m^2), and both coefficients being significant (*T*-test, p<0.0001). This conclusion involves combining the results of the two series.

To build a brightness model, it is very important to analyse the response tendencies of the individual observers to exclude observers with contradicting response tendencies before modelling. To do so, Spearman's rank correlation coefficient was calculated between the signal values of the test stimuli (Table 2) and the brightness rating values of every observer separately. The minimum, maximum, and average values of these rank correlation coefficients among all participating observers are shown in Table 4.

As can be seen from Table 4, there is positive correlation at average between the brightness ratings and the signals of all three shorter-wavelength mechanisms (*ipRGC, S, R*) as well as $\Phi_{rel,\ blue}$, but the correlation with the $|L–M|$ signal is at average negative. Considering the maximum and minimum values of the correlation coefficients, some of the observers contradict the main trend of perception of greater brightness with an increased spectral content of blue at equal luminance. In the framework of the present article, we decided to model only those observers (the majority) who follow the main trend. Similar findings of individual differences of brightness perception have also been found in liter-

Table 3. Average Values and Average Absolute Deviation Values of the Brightness Difference Ratings of All Observers (Fig. 3)

		Average brightness difference rating				**Average absolute deviation among all observers**			
	Series	**1st**	**2nd**	**1st**	**2nd**	**1st**	**2nd**	**1st**	**2nd**
No.	$\Phi_{rel,\ blue}$	267.6 cd/m^2	267.6 cd/m^2	24.8 cd/m^2	24.8 cd/m^2	267.6 cd/m^2	267.6 cd/m^2	24.8 cd/m^2	24.8 cd/m^2
13	1.164	3.0	3.5	3.0	2.5	1.0	0.5	1.0	1.5
11	0.793	2.0	2.0	3.0	2.0	1.0	1.0	1.0	1.5
4	0.74	3.0	3.0	3.0	2.0	1.0	1.0	1.0	1.0
5	0.703	3.0	2.0	2.0	1.0	1.0	2.0	1.0	1.0
7	0.652	2.0	2.0	2.0	2.0	1.0	1.5	1.0	1.0
17	0.626	2.0	2.0	2.0	3.0	1.0	1.0	1.0	1.0
19	0.414	3.0	2.0	2.0	1.0	1.0	2.0	1.0	2.5
8	0.409	1.0	1.0	1.0	1.0	1.0	0.5	1.0	0.0
20	0.381	2.0	1.0	2.0	2.0	1.0	1.5	1.0	1.0
9	0.307	0.0	0.0	0.0	0.0	0.0	0.0	0.0	0.0
15	0.274	–1.0	–1.0	0.0	0.0	0.0	0.5	0.0	0.5
16	**0.25**	**0.0**	**0.0**	**0.0**	**0.0**	**0.0**	**0.0**	**0.0**	**0.0**
14	0.238	1.0	1.0	1.0	1.0	1.0	0.0	0.0	1.0
12	0.233	–1.0	–1.0	0.0	0.0	0.0	0.0	0.0	0.0
1	0.188	2.0	0.0	2.0	–2.0	1.0	3.0	1.0	2.0
3	0.158	–1.0	–2.0	–1.0	–1.5	2.0	1.0	1.0	1.0
18	0.142	–1.0	–2.0	–1.0	–3.0	3.0	2.0	2.0	1.0
6	0.1	–2.0	–2.5	–1.0	–2.5	2.0	1.5	1.0	1.0
10	0.062	–1.0	–3.0	–1.0	–3.0	3.0	1.0	3.0	1.0
2	0.058	–2.0	–2.0	–1.0	–2.0	2.0	2.0	2.0	1.0
					Average	1.0	1.0	1.0	1.0

Note to Table 3: the 20 test stimuli (see Table 2 and Fig. 2) here are re-sorted according to their relative blue spectral content (5) in descending order. No. 16: null condition stimulus (this stimulus obtained zero average subjective brightness ratings).

ature, see the general discussion below. We use the following mathematical criterion to include the result of this observer in the brightness modelling of the present article: the value of the rank correlation coefficient with the relative spectral blue content $\Phi_{\mathrm{rel,\ blue}}$ of this observer should have been greater than 0.2 in each of the four sessions.

Eighteen of 25 observers (72 %) were included in the modelling of the 1st series and fourteen out of 21 observers (67 %) were included in the modelling of the 2nd series. The brightness ratings of the last observers (18 observers + 14 observers = 32 cases) were unified according to the following reasons. The null stimulus condition gave zero average ratings for both series and both luminance levels in the case of the last observers. At 267.6 cd/m^2, there were exclusively zero ratings in case of the null condition stimulus (i.e. same brightness as the reference) in the first series, and there was only one (–1) rating, and all others equalled 0 in the second series. At 24.8 cd/m^2, there were only two (–1) ratings, and one (+1) rating in the first series and three (–1) ratings, and one (+1) rating. Mann-Whitney's *U*-test showed no significant difference of the tendency of any one of the four null condition datasets from zero (p<0.01). We compared the data sets of the 1st series and the 2nd series also for the other 19 stimuli (Table 2, one by one separately) in addition to the null condition stimulus for both luminance levels. Mann-Whitney's *U*-test did not reveal a significant difference between the trends of the 1st series and the 2nd series for any stimulus (p<0.05), which confirms that there is no significant "position bias" (i.e. differences only because observing

Table 4. Spearman's Rank Correlation Coefficients Between the Receptor Signal Values of the Test Stimuli and the Brightness Rating Values for Each Observer and Each Experimental Session

Session							
Series	**Luminance level, cd/m²**		$ipRGC_{rel}$	S_{rel}	R_{rel}	$\lvert L_{rel}-M_{rel}\rvert$	$\Phi_{rel,\ blue}$
1	267.6	Min.	–0.10	–0.06	–0.05	–0.78	–0.11
1	267.6	Max.	0.94	0.90	0.91	0.22	0.95
1	267.6	Av.	0.49	0.49	0.50	–0.43	0.50
1	24.8	Min.	–0.16	–0.19	–0.04	–0.85	–0.19
1	24.8	Max.	0.95	0.91	0.92	0.09	0.94
1	24.8	Av.	0.56	0.53	0.59	–0.52	0.56
2	267.6	Min.	–0.50	–0.36	–0.40	–0.85	–0.45
2	267.6	Max.	0.87	0.89	0.88	0.24	0.88
2	267.6	Av.	0.50	0.50	0.48	–0.42	0.50
2	24.8	Min.	–0.20	–0.17	–0.22	–0.76	–0.21
2	24.8	Max.	0.89	0.87	0.87	0.34	0.88
2	24.8	Av.	0.59	0.57	0.57	–0.50	0.58

Note to Table 4: this shows the minimum, maximum and average values of these rank correlation coefficients among all participating observers.

the reference stimulus either on the left side or on the right side).

The resulting unified data sets (at the two luminance levels) consisted of 18+14 = 32 (cases) · 20 (test stimuli) = 640 brightness ratings (integers between – 4 and 4) per luminance level. From these two data sets, two continuous brightness scales (so-called Thurstone scales [34]) were computed for the 20 light source spectra (see Table 2 and Fig. 2) at the two luminance levels. These (2×20) Thurstone scale values, i.e. visual brightness scale (*VBS*), are depicted in Fig. 4 as a function of the quantity $\Phi_{rel,\ blue}$ with modelling data points according to (7) with different values of the exponent γ.

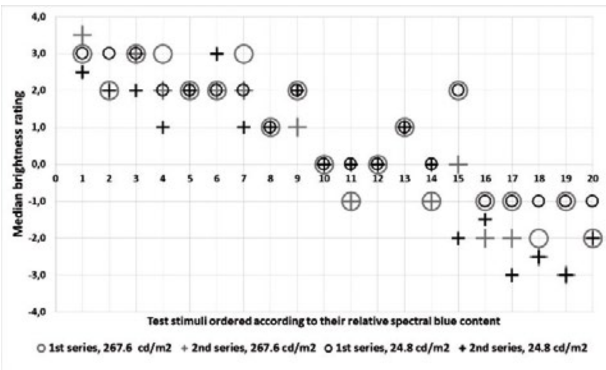

Fig. 3. The average rating on the brightness scale depending on the test stimuli, which are ordered according to their relative spectral blue content in descending order by abscissa

As can be seen from Fig. 4, the optimal values of the exponents γ according to (7) are equal 0.194 (at 24.8 cd/m^2) and 0.668 (at 267.6 cd/m^2), respectively. With these two optimal exponents, the value of Pearson's correlation coefficient (r) between the model equation (7) and the visual brightness scale was 0.925 (r^2 = 0.856) and 0.924 (r^2 = 0.853), respectively. Optimizing the exponent for the unified data set at both luminance levels, the average exponent value of γ = 0.399 came out with the following correlation coefficient values: r = 0.921 (r^2 =

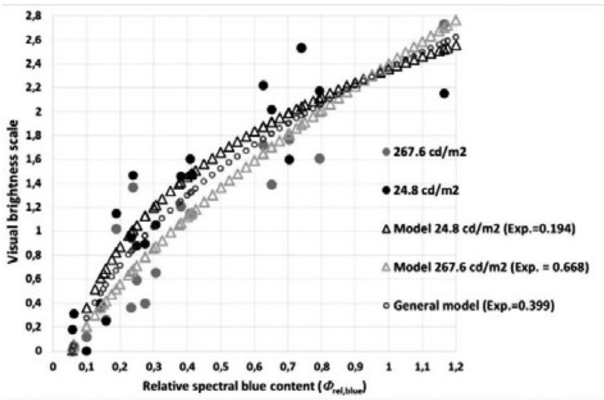

Fig. 4. Values of the visual brightness rating scale (Thurston scale) for 20 light sources at two considered luminance levels (267.6 cd/m^2 and 24.8 cd/m^2) depending on the relative spectral content of the blue colour ($\Phi_{rel,\ blue}$) of the light source, model data points are indicated according to (7) with optimum exponent values for both luminance levels and general model

Table 5. Optimum Parameter Values in Eq. (6) and Pearson's Correlation Coefficients Between the Visual Brightness Scale (*VBS*) Values and the Prediction Formula After Optimisation

Lum. level (cd/m²)		*S, ipRGC,* rods, γ	*S, ipRGC,* γ	*ipRGC,* γ	*S,* γ	*rods,* γ	*S, rods,* γ	*ipRGC,* rods, γ
267.6	γ	0.869	0.845	0.848	0.644	1.337	0.875	0.856
267.6	A_S	0.342	0.003	0	1.000	0	0.652	0
267.6	A_{ipRGC}	1.876	0.376	1.000	0	0	0	1.790
267.6	A_R	0.728	0	0	0	1.000	1.333	0.066
267.6	r	0.932	0.931	0.931	0.880	0.893	0.930	0.931
267.6	r^2	0.868	0.867	0.867	0.775	0.797	0.865	0.867
24.8	γ	0.314	0.259	0.259	0.246	0.560	0.314	0.352
24.8	A_S	0.634	0	0	1.000	0	0.285	0
24.8	A_{ipRGC}	0.000*	2.000	1.000	0	0	0	0.920
24.8	A_R	3.430	0	0	0	1.000	1.543	1.084
24.8	r	0.947	0.939	0.939	0.863	0.934	0.947	0.945
24.8	r^2	0.897	0.882	0.882	0.745	0.873	0.897	0.894

Note to Table 5: optimisation was carried out for the two luminance levels separately. Only the parameters shown in the first line were optimized; the rest were set to zero. *the value of 0.000 resulted from the optimization.

0.848) for 24.8 cd/m^2 and r=0.918 (r^2 = 0.843) for 267.6 cd/m^2, respectively. With the exponent of the Fotios and Levermore [20] model (γ = 0.24), we obtain r = 0.925 for 24.8 cd/m^2 and r = 0.909 for 267.6 cd/m^2. These correlation coefficients are not significantly different [35] from the previously mentioned values, neither in case of the optimum exponent values nor in case of the average value of γ = 0.399 (p > 0.78). If we use (B/L) from eqs. (2) and (3), we obtain r = 0.711 for 24.8 cd/m^2 (p = 0.04, significantly less than with (7) with γ = 0.399) and r = 0.815 for 267.6 cd/m^2 (p = 0.21, not significantly less than with (7) with γ = 0.399). Fig. 5 shows the dependence of the value of r^2 on the value of the exponent γ.

As can be seen from Fig. 5, the dependence of r^2 on γ is rather flat. The difference between the correlation coefficients corresponding to the average exponent value (γ = 0.399) and a specific exponent value (0.194 at 24.8 cd/m^2 or 0.668 at 267.6 cd/m^2) was not significant (p > 0.9) [35]. Therefore, it seemed reasonable to use the average exponent value (γ = 0.399) for both luminance levels in (7).

Regarding the formula for the combination of (6) first, the coefficient $A_{L–M}$ was set to zero because the correlation coefficient with the |$L–M$| signal was negative, at least within the above mentioned main group of observers that were considered for modelling in the present article. The role of the |$L–M$| signal is further analysed in section 4. The correlation coefficient between the visual brightness scale values and the prediction formula of (6) was maximized by optimizing the values of γ, A_S, A_{ipRGC} and A_R for the two luminance levels separately. Optimization was also performed by setting some of the parameters from the set {A_S, A_{ipRGC}, A_R} to zero and optimizing only the remaining parameters. Results are shown in Table 5.

As can be seen from Table 5, the obtained values of the correlation coefficient do not differ much. The significance test [35] showed no significant difference among the correlation coefficients (p>0.14 at 24.8 cd/m^2 and p > 0.38 at 267.6 cd/m^2). At the next step, the standalone *ipRGC* signal with an average exponent value (γ = 0.399) of the relative spectral blue content ($\Phi_{rel, blue}$) model of eq. (7) was considered for predicting the results with the simplest possible model. The correlation coefficients with γ = 0.399 were not significantly less (p > 0.85) than those resulting from the optimum exponent values in the 5th column of Table 5 (r = 0.922 instead of r = 0.931 at 267.6 cd/m^2 and r = 0.938 instead of r = 0.939 at 24.8 cd/m^2). These correlation coefficients are also not significantly greater than those of the $\Phi_{rel, blue}$ model with γ = 0.399. This means that based on the present visual brightness scale results, we cannot distinguish between the three shorter-wavelength mechanisms, and we cannot tell whether rod contribution can be neglected. Anyway, the optimal rod coefficients were greater

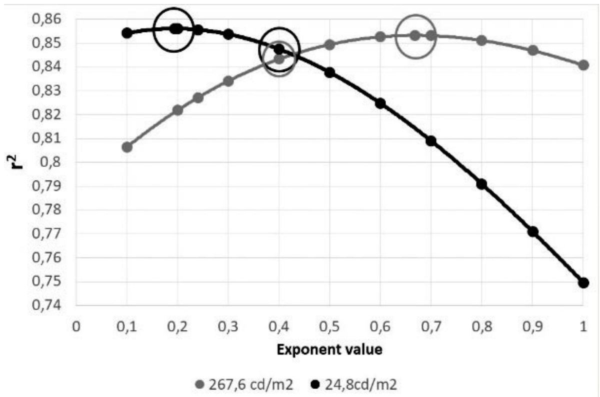

Fig. 5. Dependence of the value of Pearson's correlation coefficient squared (r^2) between visually scaled brightness *VBS* (at 24.8 cd/m^2 and at 267.6 cd/m^2) and the predicting quantity of (7) on the value of the exponent γ in (7), circles indicate optimum value pairs of r^2 and γ

at 24.8 cd/m^2 than at 267.6 cd/m^2 compared to the magnitude of the *S*-cone and *ipRGC* coefficients. This points towards the direction of rod influence at 24.8 cd/m^2. Consider that the chambers were large enough (2×41°) to cover a large retinal area, including the area of highest rod density.

According to the above analysis, the quantity *M* is proposed as the resulting brightness model of the present article that contains the average exponent value $\gamma = 0.399$:

$$M = lg\left(L_v\right) \cdot \Phi_{rel,blue}{}^{0.399}. \tag{13}$$

4. GENERAL DISCUSSION

The average model (13) that contains the relative spectral blue content and the log-luminance of the stimulus was found to be able to predict the visual brightness result with reasonable accuracy, i.e. with r=0.921 and r=0.918 at 24.8 cd/m^2 and at 267.6 cd/m^2, respectively. In the experiment, the stimulus was the light of the light sources (Table 2) reflected from the white uniform bottom of the viewing chambers (Fig. 1), and the modelling was based on this stimulus. This white stimulus can be considered as the "working point" of the visual system at the time of the brightness assessment. This white point determined the efficacy of each neural mechanism that contributes to perceived brightness.

An important limitation of the present study is that the description of the luminance dependence of brightness by lg(L_v) in eq. (13) remains a hypothesis because the two luminance levels were fixed in the present brightness experiment. Several brightness models, (1) and (2), assume a linear dependence on luminance and claim (according to the concept of equivalent luminance) to predict only whether one stimulus is brighter than another, and do not claim to predict the absolute perceived magnitude of brightness. The lg(L_v) term (instead of L_v) represents one possible way of describing luminance signal compression in the human visual system with the aim of predicting the absolute magnitude of brightness perception, and not just the order of different stimuli according to their brightness.

Another limitation of the present results is that only a part of the responses was modelled. Although this part includes the majority of the observers (about 70 %), the remaining observers did not follow the trend modelled by (13): either they had no correlation with any one of the signals, or they had low correlation with the |*L*–*M*| signal. Indeed, in a study on brightness perception, observers could be clustered into groups depending on whether their impression of brightness affects their relative spectrum at equal luminance or not [16]. Other authors also found substantial inter-observer variability of brightness perception [36–39] and pointed out that there are at least two main types of observers according to their brightness perception: a mainly chromatic type (having greater chromatic sensitivity in the entire visible wavelength range) and a mainly achromatic type (having approximately the sensitivity of the luminance channel predicted by $V(\lambda)$).

Fig. 5 in the work of Ikeda et al. [36] shows that the variation of the observers between these two main types is continuous, i.e. there are "strong", "medium" and "weak" chromatic types. Figs. 3 and 4 in the work of Ikeda et al. [36] reveal two further variants: a chromatic variant with less blue sensitivity than the main chromatic type, and an achromatic variant with even less sensitivity to blue and red than predicted by the luminance channel. The physiological reason may be that the chromatic observer has greater contribution to perceived brightness from the chromatic channels of the visual system than the achromatic observer. Another reason of the large inter-observer variability of brightness perception may be the difference in the psychological attitude of the subjects the course of the brightness discrimination experiment: achromatic observers tend to isolate the chromatic component of brightness mentally and do not respond to it.

A further question is whether the results of the present experiment is applicable to a real scene because only uniform fields were compared. Previous research indicated that" the presence of coloured objects or surfaces in the target field does not significantly affect the outcome of brightness matching trials" [40]. If, however, there was a spatially extended highly chromatic Mondrian array in the field of view, brightness evaluation was different from achromatic environments [41]. Possibly, highly chromatic images with very saturated red and orange surfaces evoke very strong red-green opponent (*L–M*) signals that contribute to their brightness and this cannot be described by such spatial brightness models that do not contain a dependence on the (*L–M)* signal. In eq. (6), with a non-zero value of the coefficient $A_{L–M}$ and also in Fotios and Levermore model [13], both chromatic channels ($|L–M|$ and $|L+M-S|$) are active so that, increasing the signals of both channels, brightness increases. If there are (several spatially extended) red and/or orange objects in the scene then we shall get higher values of the $|L–M|$ signals in the field of view and then, in turn, the contribution of the $|L–M|$ channel to the overall spatial brightness perception of the scene might become more explicit.

When combining the signals of the retinal mechanisms to predict spatial brightness in terms of retinal mechanisms, we used the standalone *S* signal instead of $|(L+M)-S|$ for the following mathematical reason. The spectral sensitivity function of the $|(L+M)-S|$ signal spectrally overlaps with the spectral sensitivities of both $|L–M|$ and luminance (*L+M*), and in general this counteracts successful parameter optimization in eq. (6). Note that in the present brightness experiment, the value of (*L+M*) was approximately constant, because luminance was constant. When optimizing 20 multi-LED spectra, the luminance signal (*L+M*) was represented by the quantity of conventional 2° photopic luminance (in cd/m^2 units) for modern applications (since this is the conventional luminance definition is most widely used today). We did not consider the alternative representations [42] of the signal of the luminance channel.

As for the adaptation time in the brightness experiment, subjects first adapted 15 minutes to the reference at the current luminance level (267.6 cd/m^2 or 24.8 cd/m^2). After this, the luminance level did not change during a session, and the subject had 40 s, during which the mixed adaptation between a test chromaticity and the reference chromaticity was established by looking slowly (i.e. for at least 2 s at each chamber) back and forth between the test and the reference chambers. The *L*-, *M*-, *S*-cone photoreceptor component of chromatic adaptation has a half-life of only (40–70) ms [43], so that a stay in each chamber for 2 s provided ample time for the chromatic cone signals to stabilize and, subsequently, for the subject to get an impression about the brightness change between the two chambers. The *ipRGC* channel, however, is much slower (with typical light adaptation times of about (100–200) s, see Fig. 3 in [44]), so we surely need a longer observation period than in the present experiment to obtain a significant *ipRGC* contribution to perceived brightness. In the practice of lighting, subjects usually spend several hours in the same visual environment, such as an office or living room. Therefore, as a validation, we need to study the brightness field in realistic viewing conditions.

The model equations (6) and (7) of this article multiply the hypothetical dependence of brightness on luminance $lg(L_v)$ depending on a shorter-wavelength sensitive signal, the relative spectral blue content ($\Phi_{rel,\ blue}$ for ≤520 nm), or a combination of S_{rel}, $ipRGC_{rel}$ and R_{rel} signals. The dependence of modelling accuracy on the exponent γ was rather low (see Fig. 5), with the most probable exponent values ranging (0.15–0.50) (in accordance with previous models), and a representative exponent value of 0.399 was adopted in the model of eq. (13). An alternative modelling hypothesis might be that the dependence of the visual brightness scale (*VBS*) on luminance should not be multiplicatively re-scaled, but additively modified by compressed and combined relative signals of *S*, *ipRGC,* and rod mechanisms:

$$VBS = lg\left(L_v\right) + A \cdot lg[A_S\left(S_{rel}\right)^{\gamma} + A_{ipRGC}\left(ipRGC_{rel}\right)^{\gamma} + A_R\left(R_{rel}\right)^{\gamma}]. \qquad (14)$$

The model (14) compresses the combination of the signals a second time by the aid of the second lg function. Neither the additive concept, nor the double-compression in eq. (14) turned out to be useful during the modelling of the present results. Therefore, we suggest the model (13) to describe the present visual data also for further validation studies. An advantage of eq. (13) is that it is easy to use in modern lighting engineering practice according to the following. For a representative set of 302 light source spectra of widely used light sources today (including LED lamps and luminaires, compact and tubular fluorescent lamps, and incandescent lamps), the relative spectral blue content ($\Phi_{rel,\ blue}$) could be approximated with reasonable accuracy ($r^2 = 0.91$) from the standard 2 ° CIE y chromaticity coordinate like

$$\Phi_{rel,blue} = -2.4174 \cdot y + 1.1405. \qquad (15)$$

The practical significance of the present brightness model is that the spatial brightness impression of real scenes (e.g. a street or a built interior) is very important in interior and outdoor lighting applications. In outdoor lighting, a higher brightness impression is associated with a better feeling of safety [6] and better obstacle detection performance. In interior lighting, a higher brightness impression of a room is associated with better work performance [45]. For architectural and lighting engineering applications, it is important to note that we cannot describe spatial brightness impression only by standard photometry, i.e. by the quantity of luminance (L_v, cd/m^2) [11–17]. Hence, we must offer a practical way to describe brightness based on basic psychophysical research. In the most typical everyday situation, a lighting specialist has a tool, and this tool can measure the luminance and chromaticity coordinates of CIE1931 (x, y). Equations (13) and (15) provide a usable brightness approximation based on the present experimental data set.

Indeed, if the lighting practitioner measures some characteristic values of the luminance (L_v) and the chromaticity coordinate y in the field of view (e.g. in the middle of a wall in a room), it will be possible to obtain a characteristic value of brightness that now depends not only on the luminance, but also on the shorter wavelength content of the spectrum, according to the present experimental results. Thus, the practical significance of the present research is that we provide lighting engineers, practitioners, and designers with the easy-to-use equation (13) by substituting eq. (15). This is ready for a real app to predict the spatial brightness of the scene. To do this, we do not need difficult apparatus. We just need a hand-held colorimetric device to read the values of L_v and y at a characteristic point to get a characteristic value of the spatial brightness prevailing in a given scene. We can also use illuminance (E_v in lx) instead of luminance (i.e. substitute L_v by E_v) and compute an illuminance-based descriptor. To measure E_v and y, we just need a hand-held illuminance-type colourimeter with a well-characterized sensor head.

Finally, we would like to further discuss in what sense the term "spatial brightness" is used, and distinguish this term from another concept. Our goal is to obtain a descriptor of the spatial brightness impression of a scene for the better visibility of small structures, textures and colour shadings on object surfaces and a better acceptance of the appearance of a built environment (e.g. a room) for interior lighting. These are important design goals in the practice of light engineer and light designer. If we increase the average luminance level of a scene (e.g. from 0.3 cd/m^2 to 3.0 cd/m^2 in street lighting or from 30 cd/m^2 to 300 cd/m^2 in interior lighting), then, regardless of the spatial structure of the scene, the overall impression of brightness of the spatially expanded scene (the so-called "spatial brightness") will increase. As mentioned in the introduction, brightness in this sense depends not only on luminance, but also on chromaticity, especially on the "shorter wavelength content" of the light source spectrum. And the lighting of a spatially extended scene with a higher correlated colour temperature (higher shorter wavelength content) results in higher perceived spatial brightness [5, 12, 13, 17, 20, 41].

This article is devoted only to this so-called spatial brightness. We are not concerned with predicting the impression of lightness of certain spatially restricted objects within a scene. To elucidate this, look at a sheet of white paper (with a several small, complicated symbols written with very thin lines and e.g. a small red strawberry image printed on it) in a well-illuminated room under the luminaire. The paper will look white. If we take this sheet in the same room into the shadow of a cupboard, the paper continues to look white, although its luminance becomes much lower. But it will be more difficult to figure out the symbols, and the red strawberry will become less brilliant, because the visual system obtains a less absolute amount of light and it does no more operate at an ideal "working point". If, in turn, we decrease the electric power of all luminaires in the room, the impression of the entire room will become dim and unacceptable, because the overall spatial brightness in the room will become low, independent of the lightness of the individual objects. Subjects entering this room will not like its appearance, because the spatial (colour) structures on the object surfaces tend to vanish, for example, the detailed structure of the faces and hair of subjects sitting in the room usually becomes less noticeable. The spatial brightness experienced in the room decreases. This effect does not depend on the structure of the scene and does not depend on the perceived lightness [46] of the individual objects in the room, as well as the simultaneous contrasts between these objects. The present article deals only with spatial brightness in the above sense.

5. CONCLUSIONS

In a visual experiment, the perception of the brightness of a large (41°) uniform field was studied. One chamber of a double-chamber viewing booth was illuminated by 20 different light source spectra at 2 different luminance levels. The other chamber contained a reference light source. The subjects had to compare the perceived brightness of the test stimuli with the perceived brightness of the reference spectrum at equal luminance. To model the mean subjective visual scale of brightness, the signal values of different retinal mechanisms (*S*-cones, rods, *ipRGCs* and the $|L–M|$ mechanism, eq. 6) plus the so-called relative spectral blue content ($\Phi_{rel,\ blue}$, the spectral radiance of the stimulus integrated for ≤ 520 nm; relative to its luminance, eq. 7) were used. Our hypothesis was that brightness depends on the logarithm of luminance, which is multiplied by either $(\Phi_{rel,\ blue})^{\gamma}$ (7) or a combination of the weighted and compressed signals of the retinal mechanisms (6).

Based on the psychophysical results, the opponent signal ($L–M$) was excluded from the model ($A_{L–M} = 0$). Accuracy of modelling of the standalone signals of the *S*-cones, rods and *ipRGCs,* as well as their combinations according to different weights in eq. (6) did not differ significantly from each other, nor did they differ significantly from the accuracy of modelling the relative spectral content of the blue colour (7). Consequently, it was not possible to decide whether rod contribution in the two experiments based on the present result could be ignored. It should be noted that in the brightness experiment, optimal rod coefficients were greater at 24.8 cd/m^2 than at 267.6 cd/m^2 compared to the magnitude of the *S*-cone and *ipRGC* coefficients. This implies the possible rod influence in case of the large uniform field of view of the brightness experiment at 24.8 cd/m^2.

Modelling quantity *M* (13) may describe the average trend of the visual brightness scale with reasonable accuracy. Eq. (13) it is easy to implement in modern lighting engineering practice, because, in addition to luminance, only the quantity relative spectral blue content ($\Phi_{rel,\ blue}$) is used, and this can be easily approximated from the *y* chromaticity coordinate according to eq. (15).

REFERENCES

1. Commission Internationale de l'Éclairage. e-ILV. Available from http://eilv.cie.co.at/, 2014.

2. Rea M.S. The what and the where of vision lighting research. Lighting Research and Technology, 2018. V50, #1, pp. 14–37.

3. Stiles WS. The Eye, Brightness and Illuminating Engineering. Transactions of the Illuminating Engineering Society, 1952. V17, pp. 241–264.

4. Robinson W. Brightness Engineering. A.M.I.E.E. Transactions of the Illuminating Engineering Society, 1951. V16, pp. 61–85.

5. Fotios SA, Cheal C. Predicting lamp spectrum effects at mesopic levels. Part 1: Spatial brightness. Lighting Research and Technology, 2011. V43, #2, pp. 43–157.

6. Rea MS, Bullough JD, Brons JA. Parking lot lighting based upon predictions of scene brightness and personal safety. Lighting Research and Technology, 2015. V49, #3, pp. 293–304.

7. Fotios S, Atli D. Comparing Judgments of Visual Clarity and Spatial, Brightness through an Analysis of Studies Using the Category Rating Procedure. LEUKOS, 2012. V8, #4, pp. 261–281.

8. Jones LA. Colourimetry: Preliminary Draft of a Report on Nomenclature and Definitions. Journal of the Optical Society of America, 1937. V27, #6, pp. 207–211.

9. Optical Society of America, Committee on Colourimetry, The Science of Colour, New York, USA: Crowell, 1953.

10. Boyce P. Editorial: The paradox of photometry. Lighting Research and Technology, 2015. V47, #7, p. 767.

11. Berman SM, Jewett DL, Fein G, Saika G, Ashford F. Photopic luminance does not always predict perceived room brightness. Lighting Research and Technology, 1990. V22, #1, pp. 37–41.

12. Fotios SA. Lamp colour properties and apparent brightness: a review. Transactions of the Illuminating Engineering Society 2001. V33, #3, pp. 163–178.

13. Fotios SA, Levermore GJ. Chromatic effect on apparent brightness in interior spaces III: Chromatic brightness model. International Journal of

Lighting Research and Technology, 1998. V30, #3, pp. 107–110.

14. Besenecker UC, Bullough JD. Investigating visual mechanisms underlying scene brightness. Lighting Research and Technology, 2016. V49, #1, pp. 16–32.

15. Rea MS, Radetsky LC. Toward a model of outdoor lighting scene brightness. Lighting Research and Technology, 2011. V43, #1, pp. 7–30.

16. Vidovszky-Németh A, Schanda J. White light brightness–luminance relationship. Lighting Research and Technology, 2012. V44, #1, pp. 55–68.

17. Fotios S, Levermore GJ. Perception of electric light sources of different colour properties. International Journal of Lighting Research and Technology, 1997. V29, #3, pp. 161–171.

18. Nayatani Y. A colourimetric explanation of the Helmholtz–Kohlrausch effect. Colour Research and Application, 1998. V23, #6, pp. 374–378.

19. Burns SA, Smith VC, Pokorny J, Elsner AE. Brightness of equal-luminance lights. Journal of the Optical Society of America, 1982. V72, #9, pp. 1225–1231.

20. Fotios SA, Levermore GJ. Chromatic effect on apparent brightness in interior spaces, II: SWS lumens model. Lighting Research and Technology, 1998. V30, #3, pp. 103–106.

21. Smith VC, J. Pokorny J. Spectral sensitivity of the foveal cone photopigments between 400 and 500 nm. Vision Research, 1975. V15, #2, pp. 161–171.

22. Commission Internationale de l'Éclairage. Models of heterochromatic brightness matching. Publ. CIE118–1995. CIE Collection in Colour and Vision, 1995. V118, #2.

23. Guth SL, Massof RW, Benzschawel T. Vector model for normal and dichromatic colour vision. Journal of the Optical Society of America, 1980. V70, #2, pp. 197–212.

24. Yaguchi H, Ikeda M. Subadditivity and superadditivity in heterochromatic brightness matching. Vision Research, 1983. V23, #12, pp. 1711–1718.

25. Kokoschka S, Bodmann HW. Ein konsistentes System zur photometrischen Stralungsbewertung im gesamten Adaptationsbereich. In: Proceedings of the CIE18th Session, London, 1975.

26. Kokoschka S: Advantage of 4-components system and its application to photometer, Proc.1994 Annual Conference and International Symp of IEI Japan, Ohmiya, 1994. Pp. 55–62.

27. Stockman A, Sharpe LT. Spectral sensitivities of the middle- and long-wavelength sensitive cones derived from measurements in observers of known genotype. Vision Research, 2000. V40, #13, pp. 1711–1737.

28. Stockman A, Sharpe LT, Fach CC. The spectral sensitivity of the human short-wavelength cones. Vision Research, 1999. V39, #17, pp. 2901–2927.

29. Rea MS, Figueiro MG, Bierman A, Bullough JD. Circadian light. Journal of Circadian Rhythms 2010. V8, #1, pp. 1–10.

30. Dacey DM, Liao HW, Peterson BB, Robinson FR, Smith VC, Pokorny J, Yau KW, Gamlin PD. Melanopsin-expressing ganglion cells in primate retina signal colour and irradiance and project to the LGN. Nature, 2005. V433, #7027, pp. 749–754.

31. Commission Internationale de l'Éclairage. Publ. CIE212–2014. Guidance towards Best Practice in Psychophysical Procedures Used when Measuring Relative Spatial Brightness, 2014.

32. Ichikawa H, Tanabe S, Hukami K. Standard Pseudoisochromatic Plates for Acquired Colour Vision Defects, Part II. Tokyo, Japan: Igaku-Shoin Medical Publishers, 1983.

33. Lanthony P. The desaturated panel d-15. Documenta Ophthalmologica, 1978. V46, #1, pp. 185–189.

34. Costa M, Gaddi C. Colour Name Distances Scaled by Thurstone's Ranking Order Psychophysical Method. Journal of Vision, 2016. V16, #12, p. 824.

35. Fisher RA. On the Probable Error of a Coefficient of Correlation Deduced from a Small Sample. Metron, 1921. V1, pp. 3–32.

36. Ikeda M, Ikeda J, Ayama M. Specification of individual variation in luminous efficiency for brightness. Colour Research and Application, 1992. V17, pp. 31–44.

37. Kimura-Minoda T, Kojima Sh, Fujita Y, Ayama M. Study on Glare of LED lamp and Individual Variations of Brightness Perception. In: Proceedings of the ISAL 7th International Symposium on Automotive Lighting, 2007.

38. Nayatani Y, Sobagaki H. Causes of individual differences on brightness/luminance (B/L) ratios. Journal of Light and Visual Environment, 2003. V27, pp. 30–34.

39. Yaguchi H, Kawada A, Shioiri S, Miyake Y. Individual differences of the contribution of chromatic channels to brightness. Journal of the Optical Society of America, 1993. V10, pp. 1373–1379.

40. Fotios SA, Cheal C. Brightness matching with visual fields of different types. Lighting Research and Technology, 2010. V43, pp. 73–85.

41. Fotios S, Atli D, Cheal C, Hara N. Lamp spectrum and spatial brightness at photopic levels: Investigating prediction using S/P ratio and gamut area. Lighting Research and Technology, 2014. V47, #5, pp. 595–612.

42. Sharpe LT, Stockman A, Jagla W, Jägle H. A luminous efficiency function, V*(λ), for daylight adaptation. Journal of Vision, 2005. V5, #11, pp. 948–968.

43. Rinner O, Gegenfurtner KR. Time course of chromatic adaptation for colour appearance and discrimination. Vision Research, 2000. V40, #14, pp. 1813–1826.

44. Wong KY, Dunn FA, Berson DM. Photoreceptor Adaptation in Intrinsically Photosensitive Retinal Ganglion Cells. Neuron, 2005. V48, #/6, pp. 1001–1010.

45. Rea MS. The Trotter Paterson Lecture 2012: Whatever happened to visual performance. Lighting Research and Technology, 2012. V44, #2, pp. 95–108.

46. Land EH, McCann JJ. Lightness and Retinex Theory. Journal of the Optical Society of America, 1971. V61, #1, pp. 1–11.

47. Yamakawa M, Tsujimura S, Okajima K. A quantitative analysis of the contribution of melanopsin to brightness perception. Scientific Reports, 2019. V9, p. 7568, https://doi.org/10.1038/s41598–019–44035–3.

Xue Guo,
M. Sc., worked as a research fellow from May 2016 until June 2018 at the Laboratory of Lighting Technology of the Technische Universitaet Darmstadt, Germany. Currently (from July 2018 on) she works for the TÜV SÜD Product Service GmbH as a product specialist for luminaires and light measurement

Peter Bodrogi,
Ph.D., studied physics at the Eotvos Lorand University in Budapest, Hungary. He obtained his Ph.D. degree from the University of Pannonia in Veszprém, Hungary and his lecture qualification thesis (habilitation) from the Technical University Darmstadt in Darmstadt, Germany. He is a research fellow at the Technical University Darmstadt. His research interests concern lighting engineering, mesopic (twilight) lighting, colorimetry, colour science, visual optimisation of displays and LED lighting systems

Tran Quoc Khanh,
Prof., Ph.D. He studied from 1980 to 1985 machine engineering and technical optics before he finished his Ph.D. thesis on the spectroscopy of UV–VIS radiation sources in 1989. Between 1990–1997 and 1997–1999, he was laboratory leader and project manager for photometry, radiometry and colorimetry at PRC Krochmann and Gigahertz Optik. Between 2000 and 2006, he was technical manager for optical imaging systems at ARRI, developed a digital CMOS camera, a film scanner and a laser recorder and optimized colour image processing for cinematography and TV signal processing. In 2005, he completed his Lecture Qualified Thesis (habilitation) on colour appearance and visual performance and started his current work as a Professor for lighting technology and solid-state lighting at the Technical University Darmstadt. He is conducting research and development projects on LED lighting technology. He is also the Chairman of the International Symposium for Automotive Lighting (ISAL). He is the author of several books and scientific articles and inventor of patents on lighting technology and related subjects. He is currently Dean of the Department of Electrical Engineering and Information Technology at the Technical University Darmstadt